N86-30174

SOME NEW RESULTS CONCERNING THE DYNAMIC BEHAVIOR OF ANNULAR TURBULENT SEALS*

H. Massmann and R. Nordmann
University of Kaiserslautern
Federal Republic of Germany

The dynamic characteristics of annular turbulent seals applied in high-pressure turbopumps can be described by stiffness, damping, and inertia coefficients. This paper presents an improved procedure for determining these parameters by using measurements made with newly developed test equipment. The dynamic system seal, consisting of the fluid between the cylindrical surfaces of the rotating shaft and the housing, is excited by test forces (input), and the relative motion between the surfaces (output) is measured. Transformation of the input and output time signals into the frequency domain leads to frequency response functions. An analytical model, depending on the seal parameters, is fitted to the measured data in order to identify the dynamic coefficients. Some new results are reported that show the dependencies of these coefficients with respect to the axial and radial Reynolds numbers and the geometrical data of the seal.

INTRODUCTION

In high-pressure turbopumps different types of annular seals are used, as illustrated in figure 1. The neck or wear ring seals are provided to reduce the leakage flow back along the front surface of the impeller face, and the interstage seals reduce the leakage from an impeller inlet back along the shaft to the back side of the preceding impeller. The geometry of pump seals may be similar to that of plain journal bearings, but they have a higher clearance-to-radius ratio and normally a fully developed turbulent flow (axial and circumferential).

Besides their designed function of reducing the leakage flow, turbulent seals have the potential to produce significant forces and have a large influence on the bending vibrations of turbopump rotors. To determine more about the pump's dynamic behavior, calculation should be carried out in the design stage. For this task the machine designer needs to know the dynamic characteristics of seals as expressed by inertia, damping, and stiffness coefficients.

Different theoretical models exist to determine the dynamic seal coefficients (refs. 1 to 4), but more experimental data are needed to compare with theoretical results and to modify existing seal models. Until now only a few measured data have been available (refs. 5 to 10). The authors have developed a test procedure to find the inertia, damping, and stiffness coefficients of annular turbulent seals. First measurement results reported in earlier publications (refs. 9, 10) pointed out the usefulness of the employed method. Meanwhile a new test rig was built that has some improved measurement possibilities and interchangeable seals. However, the measurement principle did not change essentially from the first test facility.

*This research work was supported by "Deutsche Forschungsgemeinschaft", German Federal Republic.

This paper briefly reviews the theoretical seal models and describes the employed experimental procedure for the determination of the seal coefficients. Some new results are reported, pointing out the dependence of the coefficients on the rotational frequency (circumferential Reynolds number), the axial velocity of the fluid (axial Reynolds number), and the geometrical data of the seals. They are compared with predictions from theoretical models.

DYNAMIC SEAL COEFFICIENTS - THEORETICAL MODELS

Most of the existing theoretical seal models have been developed for the simplest geometry with a fluid surrounded by a cylindrical rotating part (impeller or shaft) and a cylindrical housing (fig. 1). Such annular contactless seals separate the two spaces with pressure p_E and p_A, respectively. Caused by the pressure difference $\Delta p = p_E - p_A$, the leakage flow in the axial direction is almost always turbulent with average velocity V. Because of the rotation of the shaft a velocity is superimposed in the circumferential direction.

From a rotordynamic point of view the various theoretical models usually express a relation between the radial forces acting on the rotor and the corresponding displacements, velocities, and accelerations of the shaft. If the motions about a centered position are small, the dynamic system "seal" can be modeled by a linear system with stiffness, damping, and inertia coefficients

$$-\begin{bmatrix} F_y \\ F_z \end{bmatrix} = \underbrace{\begin{bmatrix} m_{yy} & m_{yz} \\ m_{zy} & m_{zz} \end{bmatrix}}_{\underline{M}} \begin{bmatrix} \ddot{y} \\ \ddot{z} \end{bmatrix} + \underbrace{\begin{bmatrix} c_{yy} & c_{yz} \\ c_{zy} & c_{zz} \end{bmatrix}}_{\underline{C}} \begin{bmatrix} \dot{y} \\ \dot{z} \end{bmatrix} + \underbrace{\begin{bmatrix} k_{yy} & k_{yz} \\ k_{zy} & k_{zz} \end{bmatrix}}_{\underline{K}} \begin{bmatrix} y \\ z \end{bmatrix} \tag{1}$$

where $\underline{M}$ is the mass matrix, $\underline{C}$ the damping matrix, and $\underline{K}$ the stiffness matrix of the seal.

Black was the first to derive a dynamic model for short annular seals, taking into account a leakage relation for flow between concentric rotating cylinders and a fully developed shear flow $U = R\Omega/2$ (where R is seal radius and Ω shaft angular velocity) in the circumferential direction but neglecting the pressure-induced circumferential flow. His analysis and results are discussed in references 1 and 2.

Childs (ref. 3) recently applied Hirs' lubrication equation to the dynamic analysis of seals. He used a perturbation method of Hirs' equation to obtain a closed-form analytical definition for a short seal. The zeroth-order equations for the centered position lead to a leakage pressure drop relation

$$\Delta p = (p_E - p_A) = (1 + \xi + 2\sigma)\, \rho V^2/2 \tag{2}$$

with

u inlet pressure loss coefficient
σ dimensionless friction loss coefficient (L = seal length, S = radial seal clearance), $\lambda L/S$ (3)

C-3

$$\lambda = n_o R_a^{m_o}\{1 + 1/4b^2\}^{(1+m_o)/2} \quad ; \quad b = R_a/2R_c \tag{4}$$

The friction loss coefficient λ depends on the axial Reynolds number R_a and the circumferential Reynolds number R_c, respectively

$$R_a = 2VS/\nu; \qquad Rc = R\Omega S/\nu \tag{5}$$

defined with the radial clearance S and the fluid viscosity ν. The empirical coefficients n_o and m_o have to be determined by a test for the special case.

The first-order perturbation equations lead to a pressure distribution and after integration directly to the short seal dynamic coefficients

$$E = \frac{1 + \xi}{2(1 + \xi + B\sigma)}$$

$$B = 1 + 4b^2\beta(1 + m_o)$$

$$T = \frac{L}{V}$$

$$a = \sigma[1 + \beta(1 + m_o)]$$

$$\beta = \frac{1}{1 + 4b^2}$$

v_0 = initial swirl

and

$$k_{yy} = k_{zz} = \frac{\pi R\ \Delta p}{\lambda} \frac{2\sigma^2}{1 + \xi + 2\sigma} \left\{ E(1 - m_o) - \frac{(\Omega T)^2}{4\sigma} \right.$$
$$\left. x \left\{ \frac{1}{2}\left(\frac{1}{6} + E\right) + \frac{2v_0}{a} \left[\left(E + \frac{1}{a^2}\right)(1 - e^{-a}) - \left(\frac{1}{2} + \frac{1}{a}\right) e^{-a} \right] \right\} \right\}$$

$$k_{yz} = -k_{zy} = \frac{\pi R\ \Delta p}{\lambda} \frac{\sigma^2 \Omega T}{1 + \xi + 2\sigma}$$
$$x \left\{ \frac{E}{\sigma} + \frac{B}{2}\left(\frac{1}{6} + E\right) + \frac{2v_0}{a} \left\{ EB + \left(\frac{1}{\sigma} - \frac{B}{a}\right) \left[(1 - e^{-a}) \left(E + \frac{1}{2} + \frac{1}{a}\right) - 1 \right] \right\} \right\}$$

$$c_{yy} = c_{zz} = \frac{\pi R\ \Delta p}{\lambda} T \frac{2\sigma^2}{1 + \xi + 2\sigma} \left[\frac{E}{\sigma} + \frac{B}{2}\left(\frac{1}{6} + E\right) \right]$$

$$c_{yz} = -c_{zy} = \frac{\pi R\ \Delta p}{\lambda} \frac{2\sigma\Omega T}{1 + \xi + 2\sigma} \left\{ \frac{1}{2}\left(\frac{1}{6} + E\right) + \frac{v_0}{a} \left[(1 - e^{-a}) \left(E + \frac{1}{2} + \frac{1}{a^2}\right) - \left(\frac{1}{2} + \frac{e^{-a}}{a}\right) \right] \right\}$$

$$m_{yy} = m_{zz} = \frac{\pi R\, \Delta p}{\lambda}\, T^2\, \frac{\sigma\left(\frac{1}{6} + E\right)}{1 + \xi + 2\sigma}\ ; \qquad m_{yz} = m_{zy} = 0$$

They are in reasonable agreement with prior results of Black (ref. 1) when $v_0 = 0$. The expressions point out the dependence of the seal coefficients on several parameters, like operating conditions V, Ω, the fluid temperature, the friction and entry loss coefficients σ, λ, ξ with the empirical constants m_0 and n_0 and the seal geometrical data R, L, and S. It can be shown that a few dimensionless parameters are sufficient to determine the stiffness, damping, and inertia quantities. In the later discussion the two Reynolds numbers R_a and R_c are used as test parameters as well as the geometrical data for seal clearance and seal length.

In addition to equations (6), the effect of an inlet swirl is also included in Child's original paper (ref. 3), pointing out this influence especially to the cross-coupled terms. Childs (ref. 4) as well as Black (ref. 2) have also extended their analysis to finite-length seals, and Childs has continued his work by deriving expressions for seals with different housings and rotor roughnesses.

IDENTIFICATION OF THE SEAL COEFFICIENTS

The experimental determination of the inertia, damping, and stiffness coefficients of turbulent seals is possible by means of parameter identification. Working with this method, first of all the dynamic seal model with corresponding mathematical equations, particularly frequency response functions, is required.

In the measurement step test forces (input signals) are applied to the system surface in the radial direction, and the relative motions between the two surfaces are measured (output signals). From input and output signals mobility frequency response functions can be calculated.

Finally a parameter estimation procedure is applied, requiring a good correlation between analytical and measured frequency response functions.

Dynamic Seal Model

The test rig seal model consists of the fluid, surrounded by the two cylindrical surfaces of the rotating shaft and the housing, respectively (fig. 2). The shaft of the test rig is designed to be very stiff and is supposed to have only one degree of freedom concerning the rotation about the axis. On the other hand the surface of the housing is movable only in the radial direction, having the two degrees of freedom y and z.

In these circumstances the dynamic system seal can be modeled by means of the above presented inertia, damping, and stiffness coefficients. With external time dependent forces F_y and F_z applied to the seal center in the y and z directions, the equations of motion are (see eqs. (1) and (6))

$$\left[\begin{array}{c|c} m_{yy} & \\ \hline & m_{zz} \end{array}\right]\left[\begin{array}{c} \ddot{y} \\ \hline \ddot{z} \end{array}\right] + \left[\begin{array}{c|c} c_{yy} & c_{yz} \\ \hline c_{zy} & c_{zz} \end{array}\right]\left[\begin{array}{c} \dot{y} \\ \hline \dot{z} \end{array}\right] + \left[\begin{array}{c|c} k_{yy} & k_{yz} \\ \hline k_{zy} & k_{zz} \end{array}\right]\left[\begin{array}{c} y \\ \hline z \end{array}\right] = \left[\begin{array}{c} F_y(t) \\ \hline F_z(t) \end{array}\right] \tag{7}$$

Corresponding to this two-degree-of-freedom system, a total of four stiffness frequency functions exist, assembled in the complex matrix $\underline{K}_{kin}$

$$\underline{K}_{kin} = \left[\begin{array}{c|c} k_{yy} - \omega^2 m_{yy} + i\omega c_{yy} & k_{yz} + i\omega c_{yz} \\ \hline k_{zy} + i\omega c_{zy} & k_{zz} - \omega^2 m_{zz} + i\omega c_{zz} \end{array}\right] = \underline{K} - \omega^2 \underline{M} + i\omega \underline{C} \qquad (8)$$

where ω is the exciter frequency. The inverse functions of equation (8) are the mobility frequency response functions

$$\underline{H}_{kin} = \left[\begin{array}{c|c} k_{zz} - \omega^2 m_{zz} + i\omega c_{zz} & -(k_{yz} + i\omega c_{yz}) \\ \hline -(k_{zy} + i\omega c_{zy}) & k_{yy} - \omega^2 m_{yy} + i\omega c_{yy} \end{array}\right] \cdot \frac{1}{\Delta} = (\underline{K} - \omega^2 \underline{M} + i\omega \underline{C}) \qquad (9)$$

$$\Delta = \{k_{yy} - \omega^2 m_{yy} + i\omega c_{yy}\}\{k_{zz} - \omega^2 m_{zz} + i\omega c_{zz}\} - \{k_{yz} + i\omega c_{yz}\}\{k_{zy} + i\omega c_{zy}\}$$

represented by the matrix $\underline{H}_{kin}$.

Measurements of Frequency Response Functions

From the frequency response functions (8) and (9), it is easier to measure the mobilities (9). They can be obtained by picking up input and output signals in the time domain and transforming them into the frequency domain by fast Fourier transformation. The ratio of the Fourier-transformed signals leads to the frequency response. Figure 3 shows in principle the measurement equipment. The housing is excited by a hammer impact, which is equal to an impulse force as broadband excitation. The relative displacements between the two seal surfaces (housing and shaft) are measured with eddy current pickups. After amplification and an analog-to-digital conversion the Fourier analyzer calculates the frequency response characteristics. A bus system transfers the measured data to a digital computer, where the unknown seal coefficients are calculated by means of the following identification procedure.

Estimation of Dynamic Seal Coefficients by Means of Least-Squares and Instrumental Variable Method

For the estimation of the dynamic seal coefficients a least-squares procedure, improved by an instrumental variable method, has been applied. From a theoretical point of view the product of the mobility matrix $\underline{H}_{kin}$ and the stiffness matrix $\underline{K}_{kin}$ should be the identity matrix $\underline{E}$. An additional error matrix $\underline{S}$, caused by measurement noise, has to be considered if measured mobilities $\underline{H}^{M}_{kin}$ are combined with analytical stiffnessess $\underline{K}_{kin} = \underline{K} - \omega^2 \underline{M} + i\omega \underline{C}$.

$$\left.\begin{aligned} \underline{H}_{kin}\underline{K}_{kin} &= \underline{E} + \underline{S} \\ \underline{H}_{kin}\{\underline{K} - \omega^2 \underline{M} + i\omega \underline{C}\} &= \underline{E} + \underline{S} \end{aligned}\right\} \qquad (10)$$

The complex equation (10) can be rearranged into two real equations

$$\underline{H}_k^r \underline{K} - \omega^2 \underline{H}_k^r \underline{M} - \omega \underline{H}_k^i \underline{C} = \underline{E} + \underline{S}^r$$
$$\underline{H}_k^i \underline{K} - \omega^2 \underline{H}_k^i \underline{M} + \omega \underline{H}_k^r \underline{C} = \underline{0} + \underline{S}^i \tag{11}$$

corresponding to one exciter frequency. In the case of a broadband excitation we have as many equations as frequency lines. This results in an overdetermined equation system

$$\underline{A}\ \underline{X} = \underline{E}' + \underline{S}' \tag{12}$$

where $\underline{A}$ consists of the measured frequency response functions related to the exciter frequencies ω, $\underline{X}$ represents the unknown coefficients $\underline{M}$, $\underline{C}$, and $\underline{K}$, $\underline{E}'$ is a modified identity matrix, and $\underline{S}'$ is the error matrix.

Solution of equation (12) in the sense of least squares means to minimize a loss function, defined as the Euclidean norm of S'. By deriving the loss function with respect to the seal coefficients, the so-called normal equations

$$\underline{A}^T\ \underline{A}\ \underline{X} = \underline{A}^T\ \underline{E}' \tag{13}$$

are obtained. They can be used to calculate a first set of unknown coefficients $\underline{X}^1$, by the matrices $\underline{M}^1$, $\underline{C}^1$, $\underline{K}^1$, respectively. Figure 4 shows this branch on the left side. However, the use of the described procedure may fail if the noise-to-signal ratio in the measurement is too high.

Fritzen (ref. 11) has suggested an instrumental variable method that is less sensitive to noise in the measurement data and reduces the error of the identified coefficients. With matrices $\underline{M}^1$, $\underline{C}^1$, and $\underline{K}^1$ from the first step, analytical mobility functions can be calculated. Instead of the matrix $\underline{A}^T$ a new matrix $\underline{W}^T$ with instrumental variables is built up using the above-mentioned matrices $\underline{M}^1$, $\underline{C}^1$, and $\underline{K}^1$. Matrix $\underline{A}^T$ is substituted by $\underline{W}^T$, and a new set of seal dynamic coefficients can be determined with

$$\underline{W}^T\ \underline{A}\ \underline{X} = \underline{W}^T\ \underline{E}' \tag{14}$$

This procedure is repeated and after each step the actual estimation is compared with that of the last step. Measurement and model frequency response functions are also compared. The procedure stops if the correlation is satisfactory. Our experience is that the combination of the classical least-squares method with the instrumental variable method shows much better results than the least-squares procedure alone.

TEST SETUP

Figure 5 shows a cross section of the actual test rig, which was very similar to the one described in references 9 and 10. Two annular seals were integrated symmetrically in a very rigid housing. A stiff shaft, driven by an ac motor, rotated inside the housing and acted as the second part of the seals. By using metal inserts as seal construction parts, we were able to vary the seal length, the

radial clearance, and the surface structure. The shaft was fixed to the foundation via roller bearings; the housing was connected to this system by two bolt springs and eight flexible bars. Other connections between the housing and the shaft were two mechanical seals (lip rings) in the end flanges of the casing and the most important part, the water film inside the annular seals.

The hydraulic part of the test setup consisted of a centrifugal pump that fed water into the seals. Filter and slide valves regulated the flow and the temperature of the water circulation. Flexible hose pipes connected this circuit and the movable housing. With this configuration (throughput of the pump, 4.5 m^3/h; shaft speed 6000 rpm), Reynolds numbers of about 12 000 were reached in the axial direction and up to 6500 in the circumferential direction. The water temperature was kept constant at 30 °C.

Besides this mechanical part of the test setup there was the important electronic side for the data acquisition and manipulation. Three different groups of measured values can be distinguished:

(1) Data of the fluid
(2) Data of the exciter
(3) Response data of the system

Pressure, temperature, density, and viscosity characterized the fluid state. Several pressure and temperature pickups were distributed over the test plant. The fluid velocity determined from the mass flow rate was measured in the supply line, and the shaft speed was displayed by the motor control. With these all measured data needed to calculate the seal coefficients were available. The excitation force, a blow of a hammer, was registered with a piezoelectric accelerometer mounted in the hammer head. The third group of data belonged to the motion of the housing relative to the shaft. Eddy current pickups surveyed the distance between both parts of the seal without contact. Two working planes with two orthogonal measurement directions permitted the control of housing displacement (translational and rotational).

The actual data of force and displacement as functions of time were transformed to the frequency domain by a digital spectrum analyzer that calculated the transfer functions. The parameter identification itself was carried out by desktop computer (fig. 3).

ADAPTATION OF THEORETICAL CONSIDERATIONS TO TEST SYSTEM

General Remarks

As shown in equation (7) it is possible to describe the dynamic behavior of the seal with differential equations. We can do the same for the test rig, ignoring the seal fluid mechanics. With the mass of the housing (m_H = 32.5 kg), the stiffnesses of its attachment (k_{sy} = 10 kN/m; k_{sz} = 14 kN/m) and an assumed damping and stiffness matrix for the mechanical seals (k^l, c^l), the equation of motion was written in the following form:

$$\begin{bmatrix} m_H & 0 \\ 0 & m_H \end{bmatrix} \begin{bmatrix} \ddot{y} \\ \ddot{z} \end{bmatrix} + \begin{bmatrix} c^{\ell}_{yy} & c^{\ell}_{yz} \\ c^{\ell}_{zy} & c^{\ell}_{zz} \end{bmatrix} \begin{bmatrix} \dot{y} \\ \dot{z} \end{bmatrix} + \begin{bmatrix} k_{sy} + k^{\ell}_{yy} & k^{\ell}_{yz} \\ k^{\ell}_{zy} & k_{sz} + k^{\ell}_{zz} \end{bmatrix} \begin{bmatrix} y \\ z \end{bmatrix} = \begin{bmatrix} F_y \\ F_z \end{bmatrix} \qquad (15)$$

Looking at the complete test apparatus, equation (7) could be replaced with equation (15). So we are only able to measure both influences and identify only "total" parameters (fig. 6). Later on we can correct the coefficients (i.e., reduce them to the seal coefficients) by using additional information about the system. At the moment we deal with the correction terms of the mass and the attachment stiffnesses and assume the lip ring coefficients are negligible (some more comments about this appear in the last passage of the paper).

Realization of Measurements

Every measurement set consists of four frequency response functions H_{ik} because we have a two-degree-of-freedom system. As mentioned our input data resulted from multiple-impact signals in order to reach a high energy level and a good noise-to-signal ratio during the sampling. This force and the system's response were measured simultaneously and later processed in a digital Fourier analyzer. The data set obtained in this way represented a single working condition of the test system (i.e., fluid velocity, fluid temperature, and shaft speed were constant). For all measurements the shaft speed was varied between 2000 and 6000 rpm, the water volume per time was varied between 2.5 and 4.5 m^3/h, and the temperature was constant at 30 °C.

Identification Procedure

A desktop computer was used for the subsequent treatment of the measured and stored data. A program containing both the identification procedure and an in-core solver for the determinant equations with respect to the unknown coefficients was used to calculate the parameters and the fitted frequency response functions. Both functions (measurement and curve fit) could be displayed to estimate the quality of the identification algorithm (a typical readout is shown in fig. 7). The next step in data processing was to approximate the parameters for a fixed fluid velocity with dependence of the shaft speed by using polynomial equations. Only this last representation was used in finding the measurement results.

DISCUSSION OF RESULTS

The statements written down in this passage refer to figures 8 and 9. In both cases the identified values are presented as functions of the Reynolds numbers and in relation to the theory in order to compare the different seal geometries. Figure 8 demonstrates the influence of growing axial fluid velocity R_a and two seal clearances (S_1 = 0.2 mm, S_2 = 0.4 mm); figure 9 demonstrates the parameter changes for two seal lengths (L_1 = 35 mm, L_2 = 23.5 mm) and constant R_a. The following remarks are more general then those figures imply because they are influenced by further measurements not given in this paper.

Variation of Fluid Velocity and Shaft Speed

Higher shaft speed led to higher coefficients regardless of geometry. Mass and direct damping values were nearly independent of shaft speed, cross-coupled stiffness (x stiffness) and cross-coupled damping (x damping) were linearly related to shaft speed, and main stiffness was parabolically related. In the case of x-stiffness and x-damping the substantial aspect, higher gradients for higher velocities, is not as clear as the parallel shifts of the main damping and stiffness terms. The general behavior of the values is in good agreement with one of the theories (refs. 1 to 4), for both damping values (the x-damping is approximately a linear function of the shaft speed, but there is hardly an influence of the axial velocity) and the main stiffness coefficient. The inertia term and the x-stiffness differ distinctly from the expectations. According to theory the inertia term should be only slightly influenced by the velocity, and x-stiffness should show a remarkable increase with the flow.

Comparing the absolute values with the predicted parameters (calculated for our test rig with two seals, additional stiffnesses, and the mass of the housing) showed that the measurements overestimated the main stiffness (up to 15 percent) and the mass (up to 50 percent) and underestimated the x-stiffness clearly (up to 60 percent). These errors decreased with larger seal clearances and sometimes turned around. We may suppose that there could exist an optimal seal geometry with "zero error" to the theory. The measured damping values were always in good agreement with theory. The difference was within a 5 percent range. At this point we do not want to evaluate these results, but one remark should be permitted. In the case of the mass term there was a disadvantage we had to deal with: its theoretical value of about 2 kg for both seals was less then 7 percent of the additional mass of the housing. Probably the identification algorithm or the measurement system was not sensitive enough to reflect the proper values.

Influence of Seal Clearance

The good agreements between measurement and theory are evident for the examples in figure 8 for two clearances (S_1 = 0.2 mm, S_2 = 0.4 mm). In all cases the parameters followed the predictions although the results for the x-stiffness and the x-damping were better for larger clearances than for smaller one's. Increasing the clearance reduced all coefficients. The main aspects of fluid velocity and shaft speed are reproduced for all clearances.

Influence of Seal Length

The statements for seal length are the same as in the last paragraph. The behavior of all coefficients due to the shaft speed, the fluid velocity, and the seal length were comparable to the theory. Sometimes the deviations from the precalculations were slightly higher, but in general, short seals and larger clearance were in better agreement with theory than long seals and small clearances. Probably this can be explained by the pressure drop across the seal. Short seals and wide clearances produced small pressure drops and so less energy for the system's dynamic. The result was small stiffnesses and dampings, and so we were able to excite the system with the hammer easier as if there was a high pressure drop. Therefore the best measurable seal would be a short, wide annular seal.

CONCLUSIONS

From the results we can extract some tendencies, but some results do not fit into the theory for many reasons. First, the test system is complex. We only want to determine some special characteristics, and the influences of all others should be neglected or assumed to be well known in order to find out the right values. The lip rings are one great uncertainty. Some additional measurements without seal inserts and the exact application of the described method for this special case led to stiffness, damping, and inertia terms for the test setup. For example, the mass of the housing had been found out with this method with an error less than 5 percent to the weighted mass. We found setup damping and stiffness values that showed a distinct dependence on the fluid state in the lip rings (i.e., pressure and shaft speed clearly influence these parameters). But without searching for the roots of these coefficients we corrected the measured seal coefficients with them and found some interesting results:

1. The difference between theory and measurement was smaller than without the seal inserts.
2. The skew symmetry of the matrices improved.
3. The error in the mass term was constant.

The lip rings can presently be described as a conservative element with damping and stiffness attributes. But this should be verified in the near future.

The second critical remark touches the inlet swirl. We were not able to measure the circumferential velocity of the fluid at the entrance of the seal. For short seals we assumed a fully developed Couette flow with an inlet swirl of zero because of the geometric configuration of the test rig. This was not the case for longer seals, so that could explain once more some differences between theory and measurements.

REFERENCES

1. Black, H.F., "Effects of Hydraulic Forces in Annular Pressure Seals on the Vibrations of Centrifugal Pump Rotors", I.M.Eng. Sci., Vol. 11, No. 2, pp. 206-213, 1969

2. Black, H.F. and Jensen, D.N., "Dynamic Hybrid Properties of Annular Pressure Seals", Proc. J. Mech. Engin., Vol. 184, pp. 92-100, 1970.

3. Childs, D.W., "Dynamic Analysis of Turbulent Annular Seals Based on Hirs' Lubrication Equation", Journal of Lubrication Technology, ASME-Paper No. 82-Jub 41, 1982.

4. Childs, D.W., "Finite Length Solutions for Rotordynamic Coefficients of Turbulent Annular Seals", Journal of Lubrication Technology, ASME-Paper No. 82-Lub 42, 1982.

5. Childs, D.W. and Dressman J.B., "Testing of Turbulent seals for Rotordynamic Coefficients", NASA Conference Publication 2250, Rotordynamic Instability Problems of High Performance Turbomachinery, Proceedings of a workshop held at Texas A&M University, 10-12 May 1982, pp. 157-171, 1982.

6. Childs, D.W. et al, "A High Reynolds Number seal Test Facility: Facility Description and Preliminary Test Data", NASA Conference Publication 2250, Rotordynamic Instability Problems of High Performance Turbomachinery, Proceedings of a workshop held at Texas A&M University, 10-12 May 1982, pp. 172-186.

7. Iino, T. and Kaneko, H., "Hydraulic Forces by Annular Pressure Seals in Centrifugal Pumps", NASA Conference Publication 2133, Rotordynamic Instability Problems of High Performance Turbomachinery, Proceedings of a workshop held at Texas A&M University; 12-14 May 1980, pp. 213-225, 1980.

8. Kanki, H. and Kawakami, T., "Experimental Study on the Dynamic Characteristics of pump annular seals, Conference "Vibrations in Rotating Machinery", York 1984, C 297/84, IMechE 1984.

9. Nordmann, R. and Maßmann, H., "Identification of Stiffness, Damping and Mass Coefficients for Annular Seals, Conference "Vibrations in Rotating Machinery", York 1984, C280/84, IMechE 1984.

10. Nordmann, R. and Maßmann, H., "Identification of Dynamic Coefficients of Annular Turbulent Seals, "NASA Conference Publication 2338, Rotordynamic Instability Problems in High-Performance Turbomachinery 1984, Proceedings of a workshop, May 28-30, 1984, pp. 295-311.

11. Fritzen, C.-P., "Identification of Mass, Damping and Stiffness Matrices of Mechanical Systems", submitted to 10th ASME Conference on Mechanical Vibration and Noise, Sept. 85, Cincinnati

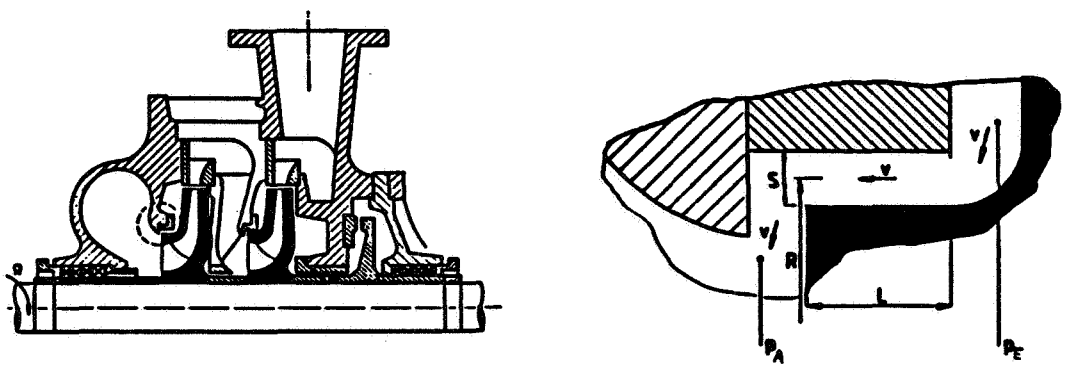

Figure 1. - Annular seal types in turbopumps.

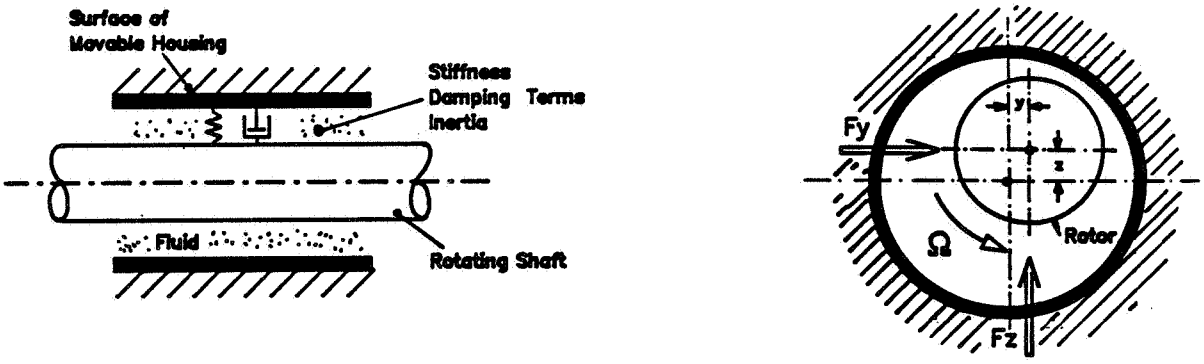

Figure 2. - Hydraulic forces in seal.

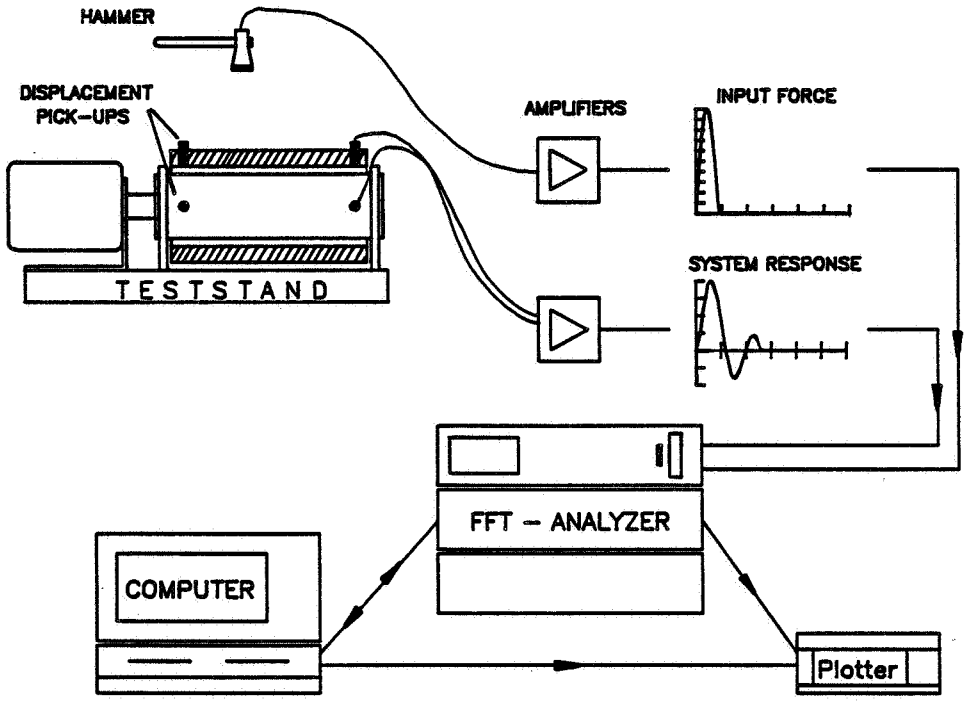

Figure 3. - Data acquisition and processing.

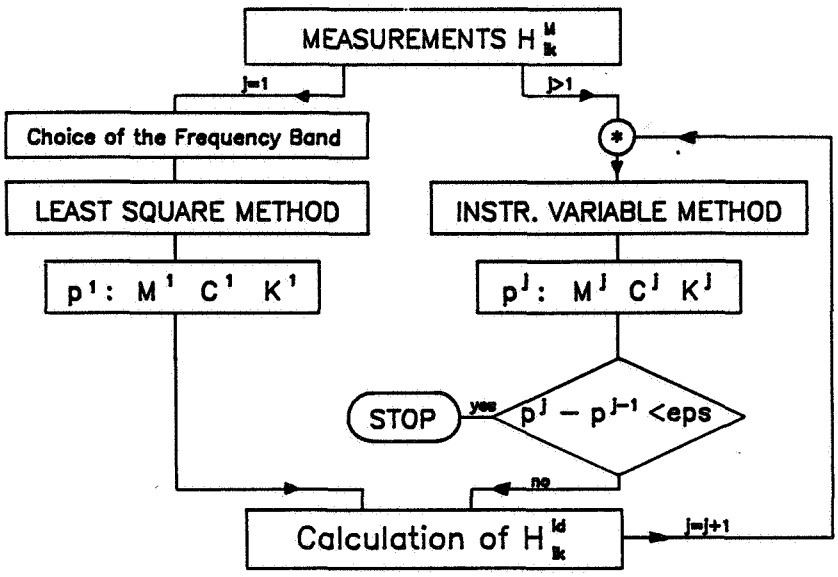

Figure 4. - Principle of instrumental variable method.

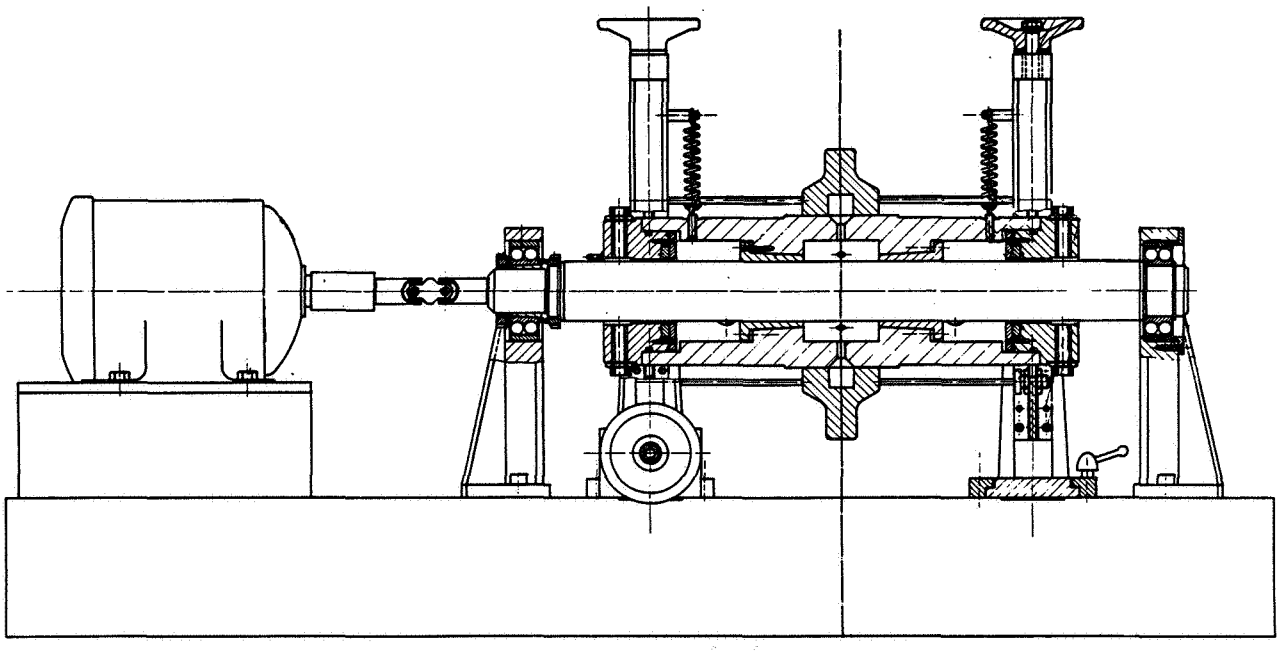

Figure 5. - Cross section of test rig.

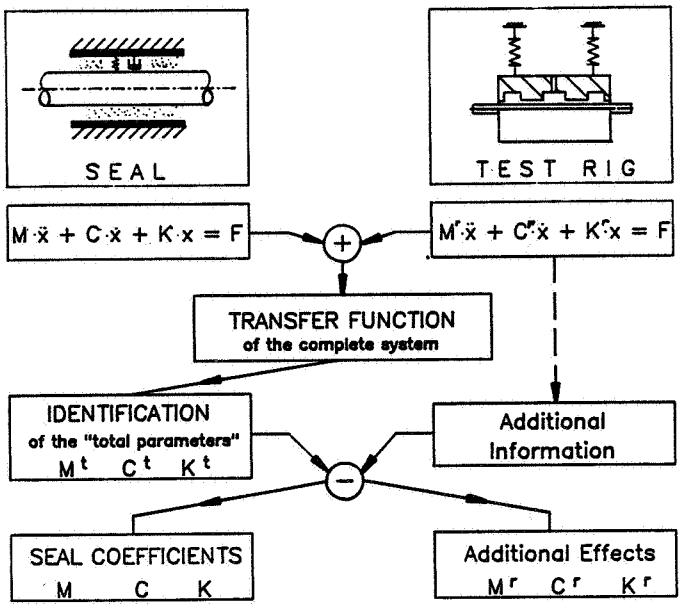

Figure 6. - Adaptation of theoretical considerations to real system.

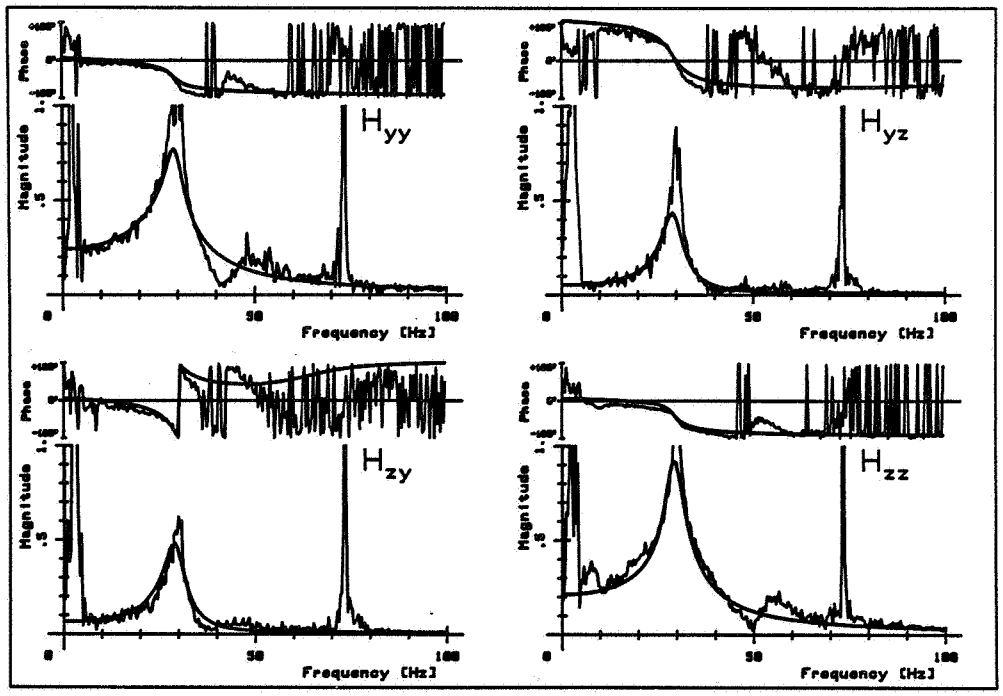

Figure 7. - Example of measurements and curve-fit data.

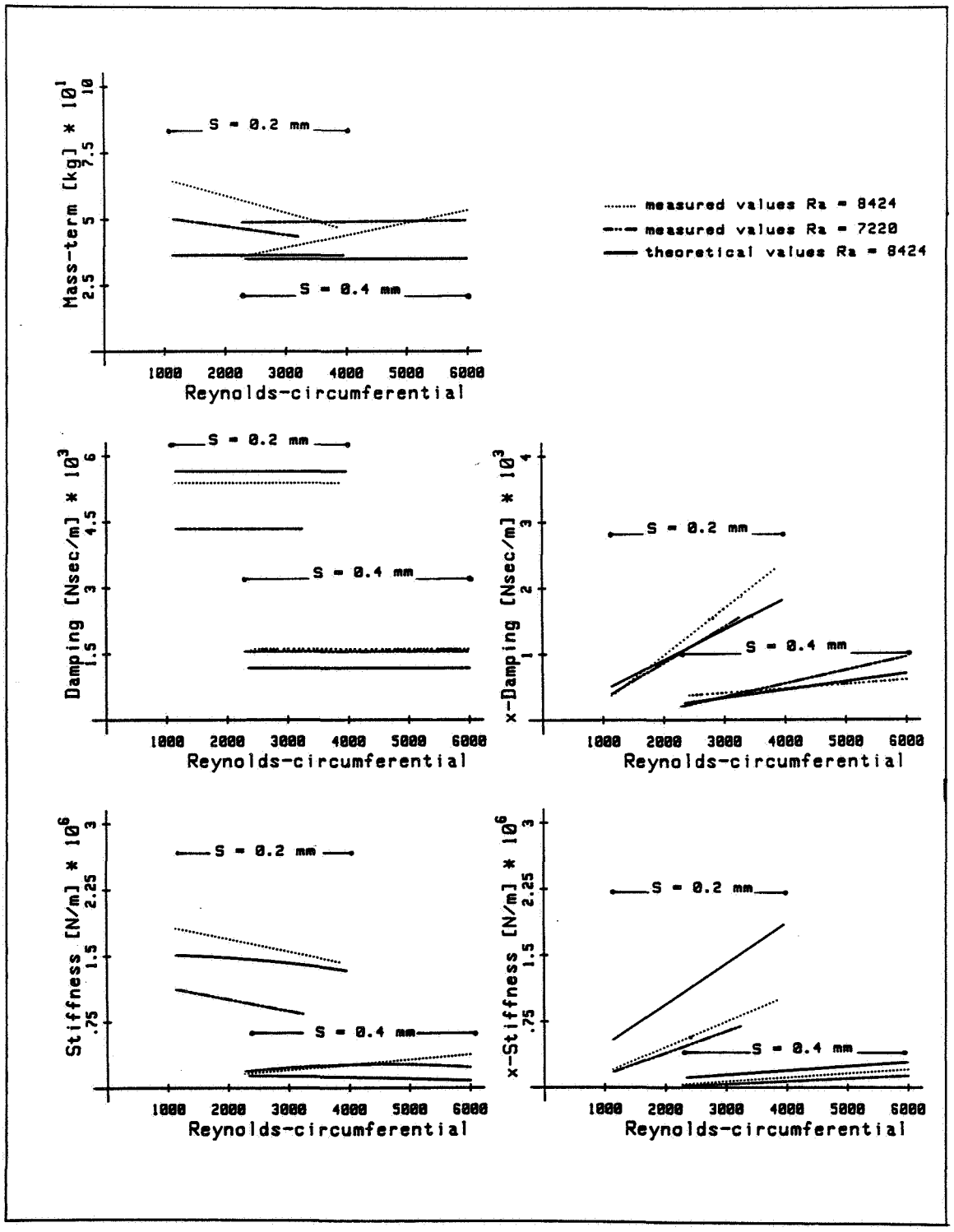

Figure 8. - Influence of seal clearance S for L = 35 mm and T = 30 °C.

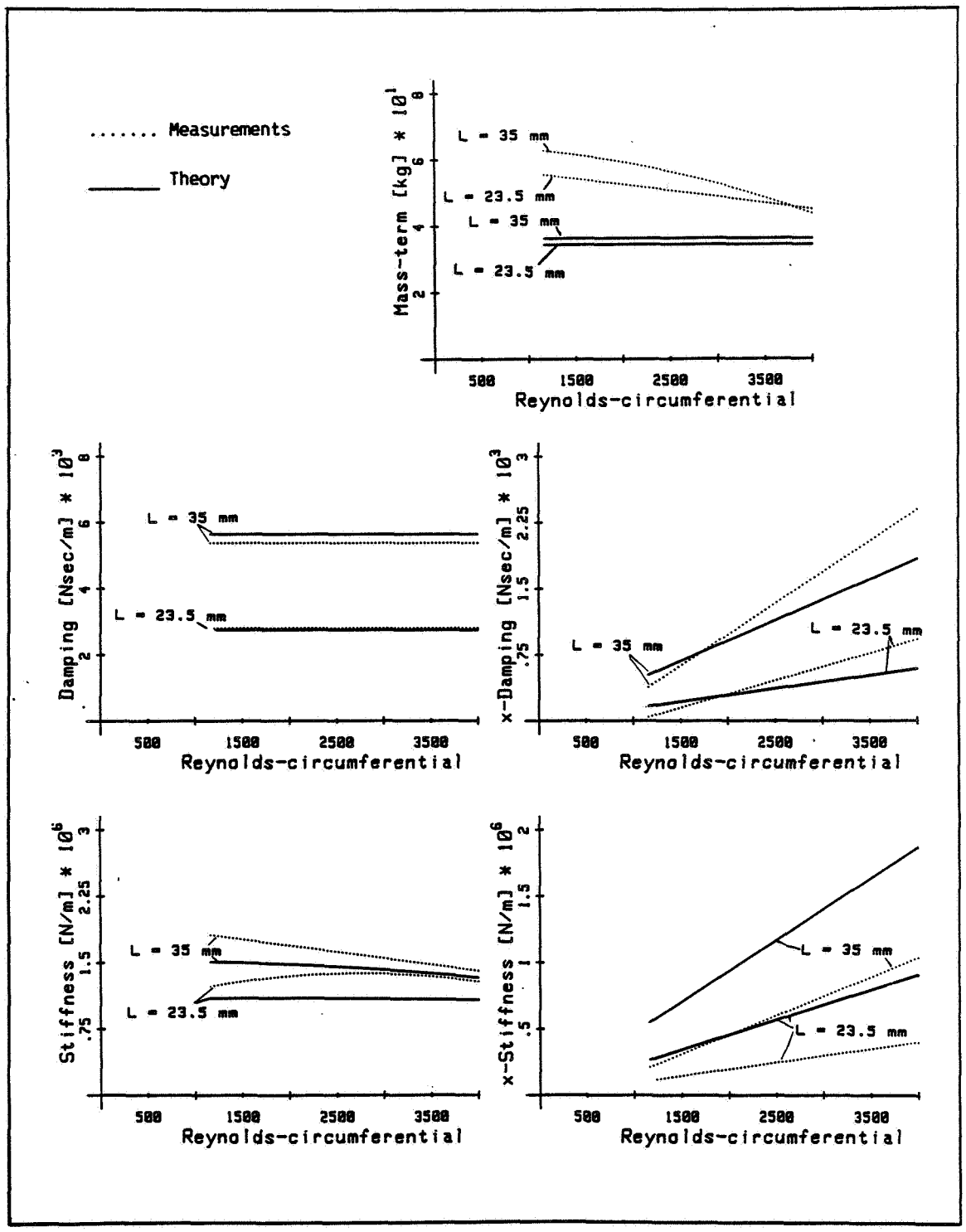

Figure 9. - Influence of seal length L for S = 0.2 mm, R_a = 8424, and T = 30 °C.